Basrah Journal for Engineering Sciences, Vol. 23, No. 1, (2023), 72-80

Original Article

Journal homepage: www.bjes.edu.iq
ISSN (Online): 23118385, ISSN (Print): 18146120

Numerical Simulation and Optimization of Friction Stir Welding Parameters

Sadiq J. Jasim [1, *], Nathera A. Saleh [2], Raad J. Jasim [3]

[1, 2, 3] *Department of Mechanical Engineering, College of Engineering, University of Basrah, Basrah, Iraq*
E-mail addresses: cfowe@outlook.com , nathera.saleh@uobasrah.edu.iq , raad.jassim@uobasrah.edu.iq
Received: 16 May 2022; Revised: 12 June 2022; Accepted: 21 June 2022; Published: 2 July 2023

Abstract

In this paper friction stir welding process has been studied whereby utilized FEM method (Ansys software ver. 20). The main effective parameter in this process were rotational speed, linear speed, tool shoulder radius, heat transfer coefficient and clamping percentage to study their influence on represent temperature, von misses stress and frictional stress distribution. Because of the difficulty to obtained the number of the simulation cases in order to get the most important results, Taguchi L27 orthogonal array was apply to reduce the total number of the simulation cases. Pure copper (t = 3.18 mm) material type was applied as work plate material. ANOVA statistical tool was utilized to achieved the optimization process after the simulation cases done. Percentage of contribution of each parameter can be obtained by ANOVA table and mean of S/N ratio plot. Validation process was achieved between the Current study and experiment work in the temperature distribution field with percentage of error 2.7 %. From optimization result It is found that the optimum condition in order to obtained good results for temperature was rotational speed of (450 rpm), linear speed (2.75 mm/s), tool shoulder radius (7 mm), heat transfer coefficient (300 w/m^2 K), clamping distance percentage (40 %). And for von misses stress was rotational speed of (550 rpm), linear speed (3 mm/s), tool shoulder radius (7 mm), heat transfer coefficient (300 w/m^2 K), clamping distance percentage (20 %). While for frictional stress was rotational speed of (450 rpm), linear speed (2.5 mm/s), tool shoulder radius (7 mm), heat transfer coefficient (300 w/m^2 K), clamping distance percentage (30 %).

Keywords: Friction stir welding, Taguchi, ANOVA, S/N ratio, Pure copper.

https://doi.org/10.33971/bjes.23.1.10

1. Introduction

The Welding Institute (TWI) invented friction stir welding in 1991. This solid-state method was first used on Al-Alloys but now it is applied to weld various materials such as Cu-alloy, Ni-alloy, Ti, and Mg. Because of the high quality of this technique, it was used to weld metals that were previously difficult to weld. The concept of friction stir welding (FSW) is based on converting mechanical energy, represented by friction between the tool and the material, into thermal energy, which is used to heat and join the metal. Plastic deformation also plays an important role in (FSW). In recent years, FSW has come to compete strongly with traditional welding methods and has expanded to include underwater welding [1] and polymer welding [2] in addition to the applications of machine learning [3] and online monitoring [4]. There are numerous researches investigated FSW experimentally and numerically. Jayaraman et al. [5] achieved an optimization process on the friction stir welding of AL319 as the work piece material to study the effect of rotational speed, welding speed, and axial force on the optimum value of tensile strength of the (FSW) joint alloy. They used Taguchi's (L27) orthogonal array with three variables and three levels. Experimental results show that rotational speed has a large effect on tensile strength but axial force has a small effect. A quadratic mathematical model was created for nonlinear regression analysis. Gök et al. [6] used AZ31 Magnesium alloy as a work piece. The simulation process is completed by utilizing DEFORM 3D (finite element package). Additionally, three levels of rotational speed and two levels of linear speed were applied in this model. Observed when the linear speed is increased, there is a decrease in maximum temperature but an increase in the material amount moved per rotation, as well as a decrease in mixer time (time required for the amount material to move from advanced side to the retreaded side) resulting in a decrease in the heat input value. Jabbari [7] employed thermal model simulation and experimental work of (FSW) with pure copper as the material plate type. Simulation process was carried out whereby COMSOL (finite element package) with three level of feed rate velocity and constant rotational speed, While the experimental work was completed with three level of rotational speed and constant feed rate velocity. Achieved from the experimental results that any increase in rotational speed at fixed value of traverse speed will cause an increase in the strength of the welding join. Gihad et al. [8] utilized experimental and finite element analysis with pure copper as the material type. Constant value of rotational speed was employed in order to determine the quality of welding joint. FEM was applied to obtained the temperature distribution and the welding stresses. Temperature and axial force data from the experiments results have been utilized in order to achieved the (FEM) validate. Sahu and Pal [9] carried out the Experiments utilizing Taguchi's L18 factorial design of experiment. The parameters of the processes were optimized using grey rational analysis. The percentage effect of each process parameter on weld quality was calculated. To make the

square but joint, they employed AM20 Magnesium Alloy. Tool rotation speed, welding speed, shoulder diameter, and plunge depth were applied as process parameters. Tensile tests were utilized after welding to determine ultimate tensile strength and yield strength. Lee et al. [10] utilized an (FEM) simulation method, the main parameters in this study were tool shoulder diameter, rotational speed and welding speed. The results show that rotational speed have large effect on the maximum temperature value as well as the increase in the mention three parameter will increased von misses stress value. Constantin et al. [11] used the (FE) code ABAQUS to simulate thermal and mechanical coupled fields. In this model constant rotation speed was employed with a plunge velocity and welding velocity. Obtained good agreement between the numerical and experimental temperature distribution results. Raheem [12] studied the optimization process whereby response surface method (RSM) in order to obtained optimum value of joint strength of the (FSW) process. The chosen parameters were welding speed, tool rotational speed, axial load and geometry of the tool. Achieved that the best method in (RSM) was central composite design (CCD) with three or four factors. According to the papers cited, rotational speed, linear speed, tool shoulder radius, heat transfer coefficient, and clamping percentage are the important parameters in (FSW). These parameters and their effects on output results which include temperature, von misses stress and frictional stress distribution as well as to obtained the optimum value from the responses whereby utilized the optimization tools like Taguchi's Design Method and response surface method (RSM) during friction stir welding simulation process have been studied.

2. Finite element modeling (FEM)

2.1. Geometrical modeling

The plate dimensions in this mode are length 70 mm, width 150 mm, thickness 3.18 mm the tool dimension, which are the tool shoulder radius, is a variable parameter with a range of 6.5-7 mm and high = 15.24 mm, as shown in Fig. 1.

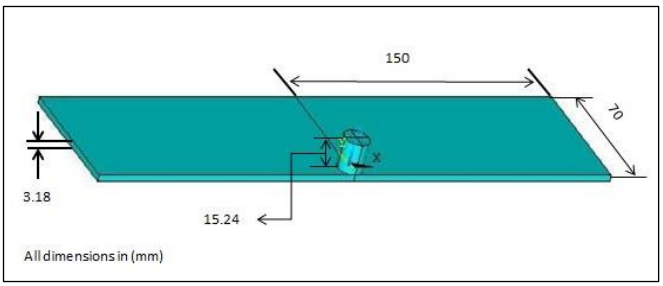

Fig. 1 geometry configuration of plates and tool.

2.2. Material properties

The pure copper (Cu 99.85 %) with the chemical combination listed in Table 1. Jabbari [7] employed in this model while tool is almost entirely made of material such as Polycrystalline Cubic Boron Nitride (PCBN) [13].

Table 1. Chemical composition of the pure copper plates.

Cu	Ni	Zn	Si	Al	Fe	Mn	B	Sb
99.85	0.08	0.041	0.007	0.006	0.006	0.006	0.002	0.001

Thermal and mechanical properties are listed in the Table 2 for the work plate and tool material [11].

Table 2. thermal and mechanical properties.

Material Properties of the Plates						
Young's modulus	120 GPa					
Poisson's ratio	0.33					
Coefficient of thermal expansion	1.875×10^{-5} μm/m°C					
Bilinear isotropic hardening constants						
Yield stress	150 MPa					
Tangent modulus	1 GPa					
Temperature dependent material properties						
Temperature (°C)	25	100	130	160	190	200
Thermal conductivity (W/m °C)	328	325	322	320	318	316
Density (kg/m^3)	8940	8895	8879	8864	8856	8840
Specific heat (J/kg °C)	385	394	397	398	401	403
Material Properties of the PCBN Tool						
Youngs modulus	680 GPa					
Thermal conductivity	100 W/m °C					
Poisson's ratio	0.22					
Density	4280 kg/m^3					
Specific heat	750 J/kg °C					

2.3. Meshing modeling for the system

2.3.1. Solid mesh modeling

In this model a coupled thermal and mechanical field is present. SOLID226, 3-D with 20-Nodes element type is used to create the geometric model of the work plate and the tool. The reason why this type of element was utilized is because of its stress stiffness and the coupled field has large strain and large deflection capabilities. To prevent oscillations in the thermal solution and nonphysical temperature distribution, a hexahedral mesh was used with mid-side nodes. In the welding tool, Pilot node was used to control the tool's movement and to apply the rotation speed on the welding tool. Figure 2 represent mesh modeling for (FSW) system.

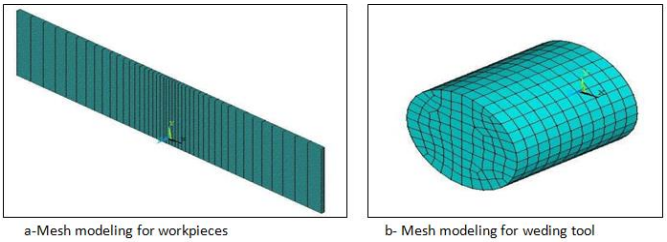

Fig. 2 mesh modeling.

2.3.2. Contact surfaces modeling

Friction stirs welding process required excellent contact between system parts so in this section there are three type of contact (plates surface contact, plates and tool surface contact, pilot node and tool surface contact). Surface element should be defined so that the element types (CONTA175) and (TARGE 174) used to perform the standard surface-to-surface contact as shown in Fig. 3. In addition, a high value of thermal contact conductivity (TCC = 2E06 W/m^2 °C) has been used to ensure continuous bonding between the workpiece material.

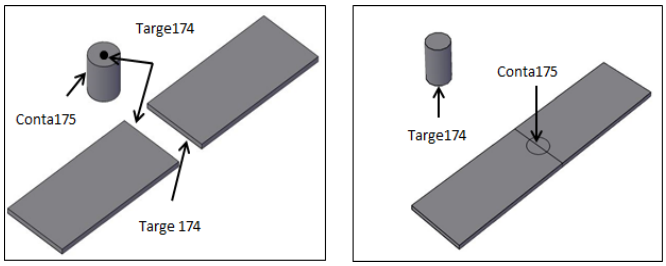

Fig. 3 contact model for (FSW) surfaces.

2.4. Mechanical and thermal boundary condition

2.4.1. Mechanical boundary condition

Work piece should be kept stationary and not move. The workpiece clamped at a variable percentage (20 %, 30 %, 40 %) and all nodes detected in this region constrained in all directions, as well as the lower surface of the workpiece in the (Z) direction as seen in the Fig. 4.

2.4.2. Thermal boundary condition

Heat generated by friction and plastic deformation will be distributed throughout the work piece. Also, some of this heat will be lost due to the tool surface in the convection method and the upper surface of the workpiece in the convection and, Hamed [14] recognizes a value for heat transfer coefficient which is in the range of (10 – 30 W/m^2 K) for the upper plate surface and tool surface so in this analysis the heat transfer coefficient is (h = 10 W/m^2 K).

$$Q_1 = h_1 \, (T_{s1} - T_{air})$$

$$Q_2 = h_1 \, (T_{s2} - T_{air})$$

$$h_1 = h_2 = 10 \ \mathrm{W/m^2\,K}$$

$$T_{air} = 25 \ ^\circ\mathrm{C}$$

Where:
Q_1: is heat transfer due to the upper surface of the plates.
Q_2: is heat transfer due to the surface of the tool.
T_{s1}: is the temperature of the upper surface of the plates.
T_{s2}: is the temperature of the tool surface.

However, the value of the heat transfer coefficient will always be large for the lowest surface of the workpiece because heat transmission from the lower portion is high due to the backing plate and heat transfer whereby the conduction method as fixed in below Fig. 4. In this analysis, the heat transfer coefficient is variable parameter and according to saad [15], three ranges (150, 300, and 450 W/m^2 K) were employed.

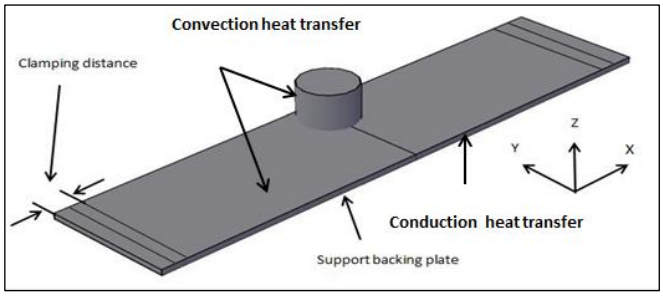

Fig. 4 thermal and mechanical boundary condition.

3. Finite element modeling validation

The FEM analysis results were confirmed by comparing them with the numerical data published in the literature Constantine et al. [11], and Fig. 5 shows the temperature contours distribution for validation case. Good agreement was obtained in the temperature distribution along 50 mm distance from the starting point as well as temperature distribution in the width direction of the plate, Fig. 6 shows the temperature plot at 50 mm distance.

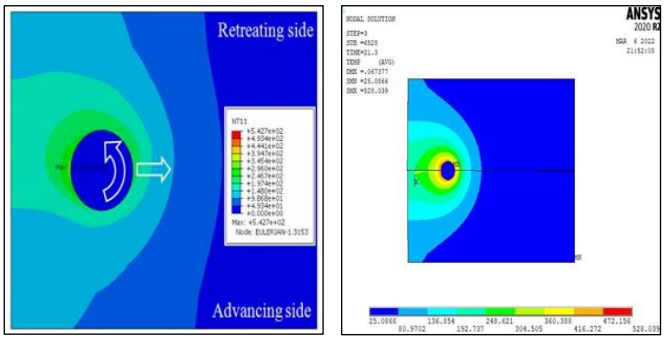

(a) Constantine [7] **(b)** Present study

Fig. 5 temperature contours distribution for the validation process.

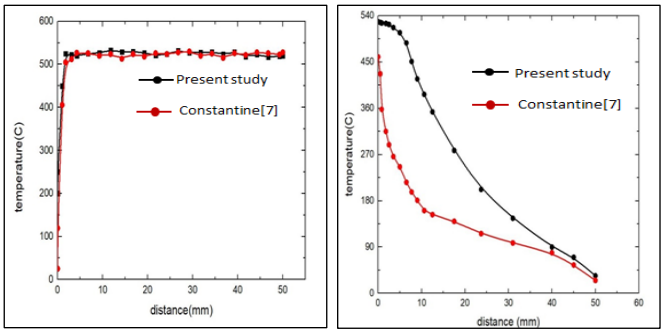

(a) Longitudinal direction **(b)** Width direction

Fig. 6 temperature plot for the validation

4. Optimization process

Optimization is a very effective and adaptable tool that applied to any engineering area. Optimization is a process that allow to improve and develop from the product properties whereby select the effect variable or decrease the value of the noise in the response. Taguchi's design method was apply in this model.

4.1. Taguchi's design method

Taguchi method is a proposed experiment and numerical which allows for the selection of the product or technique that consistently performs and to keep the variance in the output very low even in the presence of noise inputs. The Taguchi design focuses on identifying elements that reduce the noise during any process, noise can be changed and determined through testing. To build a resilient process or product, the best factors settings should be used. It will produce more consistent output regardless of the setting in which it was utilized if it is developed with this goal in mind. Orthogonal arrays with some of the selected factors and their levels were employed in Taguchi designs to evaluate the effect of each parameters on the output response. An orthogonal array focuses on a well-balanced design that gives equal weight to all parameters. This

allows for independent parameter evaluation. When fractionated designs are adopted, time and cost associated with simulate process can be decreased.

4. Results and discussion

4.1. FEM simulation results

The input parameter in this study which represent rotational speed, linear speed, tool shoulder radius, heat transfer coefficient and clamping percentage. All parameters have three value for all simulation cases which are rotational speed have (350, 450 and 550 rpm), linear speed (2.5, 2.75 and 3 mm/s), tool shoulder radius (6.5, 6.75 and 7 mm), heat transfer coefficient (150, 300 and 450 W/m^2 K) and clamping percentage (0.2, 0.3 and 0.4). Thermal and mechanical results represent in Table 3.

Table 3. thermal and mechanical results

W (rpm)	V (mm/s)	R (mm)	H (W/m^{2}K)	C	T (°C)	σ_v (MPa)	σ_f (MPa)
350	2.5	6.5	150	20	453.1	165.9	57.5
350	2.75	6.5	150	20	400.395	199.3	66.46
350	3	6.5	150	20	314.29	213.56	107.68
350	2.5	6.75	150	20	494.8051	188.42	51.44
350	2.5	7	150	20	634.45	190.61	48.72
350	2.5	6.5	300	20	392.46	194.55	89.88
350	2.5	6.5	450	20	348.2331	191.61	68.2815
350	2.5	6.5	150	30	467.35	144.8	67.5
350	2.5	6.5	150	40	281.52	136.8	63.5
450	2.5	6.5	150	20	609.96	220.3	100.26
450	2.75	6.5	150	20	493.1847	239.21	126.21
450	3	6.5	150	20	430.94	263.67	138.01
450	2.5	6.75	150	20	704.3397	255.22	69.71
450	2.5	7	150	20	843.9867	230.47	49.17
450	2.5	6.5	300	20	568.24	244.32	114.71
450	2.5	6.5	450	20	527.76	238.07	76.71
450	2.5	6.5	150	30	691.78	190.77	118.53
450	2.5	6.5	150	40	743.54	160.04	88.65
550	2.5	6.5	150	20	715.948	246.3	52.26
550	2.75	6.5	150	20	515.63	269.21	65
550	3	6.5	150	20	426.33	275.47	72.02
550	2.5	6.75	150	20	726.43	264.27	28.51
550	2.5	7	150	20	896.13	286.47	20.51
550	2.5	6.5	300	20	580.73	262.42	61.51
550	2.5	6.5	450	20	489.345	267.67	43.12
550	2.5	6.5	150	30	789.345	227.88	61.27
550	2.5	6.5	150	40	822.704	210.18	44.25

From the above Table 3, the effect of each input parameter on the output result can be obtained as following:

4.1.1. Temperature distribution

From the Fig. 7 it clear that when the rotational speed increases the value of maximum temperature during friction stir welding will raise due to the increase in the heat generation and plastic deformation which play important role in this process.

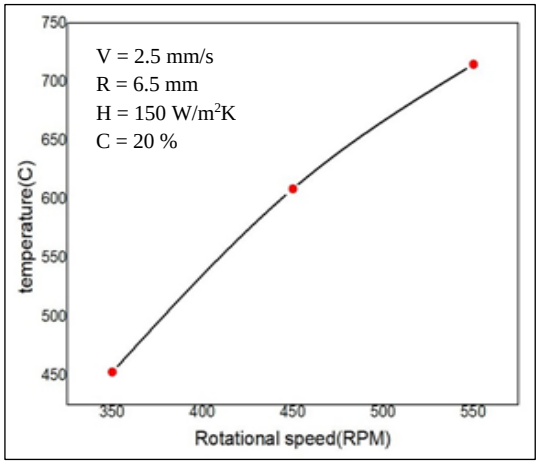

Fig. 7 temperature with rotational speed.

While the decrease in the maximum value of the temperature due to the increase in the linear speed during the FSW process because of the mixture time will reduce and according to the reduction the heat input will reduce as shown in Fig. 8.

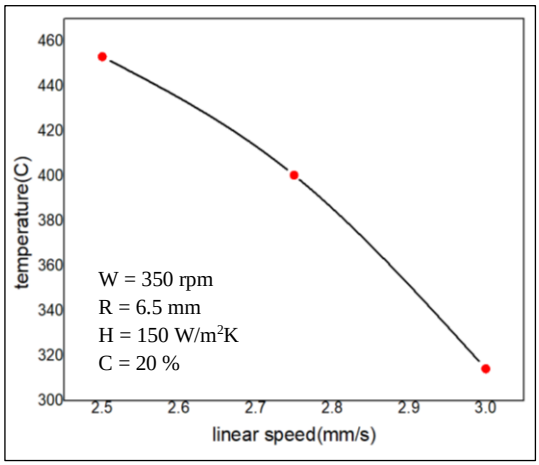

Fig. 8 temperature with linear speed.

Also, there is an increase in the value of maximum temperature as the tool shoulder radius will increase because the contact area between the tool and work plate will be high so that a good reason to obtained more heat generation in form of temperature as shown in Fig. 9.

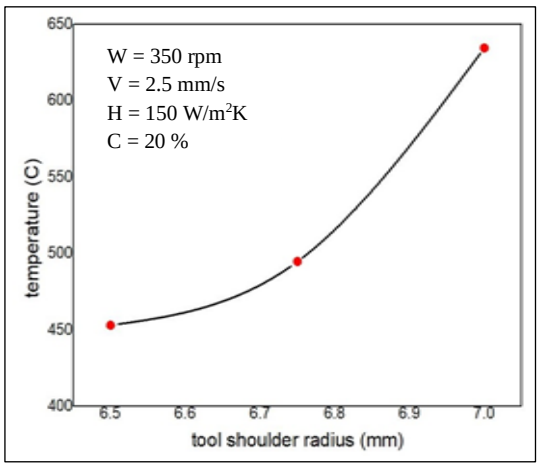

Fig. 9 temperature with tool shoulder radius.

For the heat transfer coefficient when it is increases the value of maximum temperature will dope due to the heat transfer removal as in the below Fig. 10.

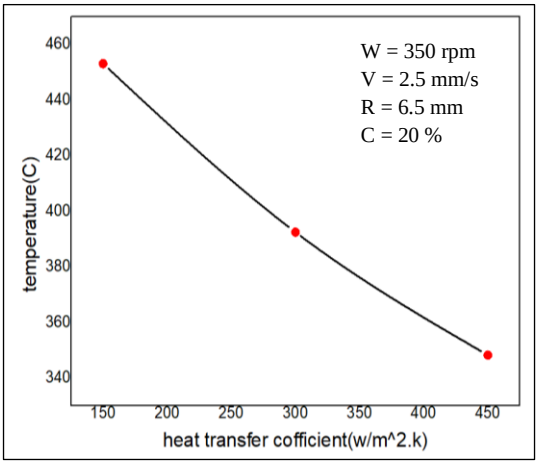

Fig. 10 temperature with heat transfer coefficient.

It is clear that from the Fig. 11 when the clamping percentage increases this will cause in increases in the maximum temperature value because it will make the contact condition continuous during the process also it will make the stability of the work plate.

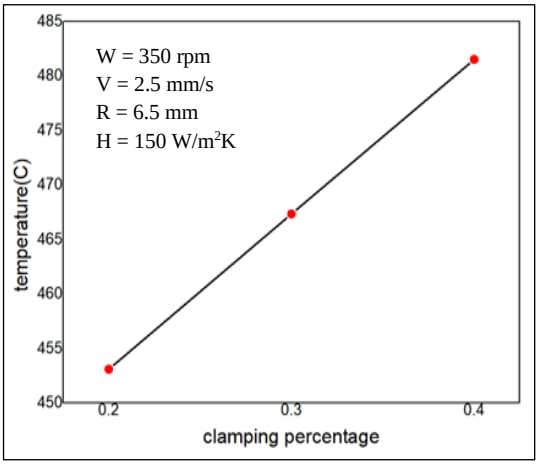

Fig. 11 temperature with clamping percentage.

Non-linear mathematical equation was obtained between the temperature (T) and the turning parameters whereby utilized the FEM results and Taguchi method for optimization as given in the equation (1).

$$T = 19907 + 13.574(W) - 6667(V) - 4422(R) + 2.076(H) - 12.8(C) - 0.01435(W^2) + 1180.8(V^2) + 362.2(R^2) - 0.00375(H^2) + 0.00673(\mathrm{W} \times \mathrm{C}) + 1.65(\mathrm{V} \times \mathrm{C}) + 1.69(\mathrm{R} \times \mathrm{C}) \quad (1)$$

4.1.2. Von misses stress

It is clear that when the rotational speed, linear speed and tool shoulder radius increases the maximum value of von misses stress will be increase as show in Figs. 12, 13 and 14.

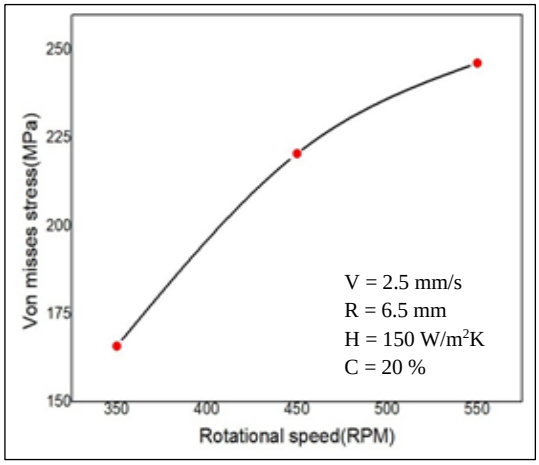

Fig. 12 von misses stress with rotational speed.

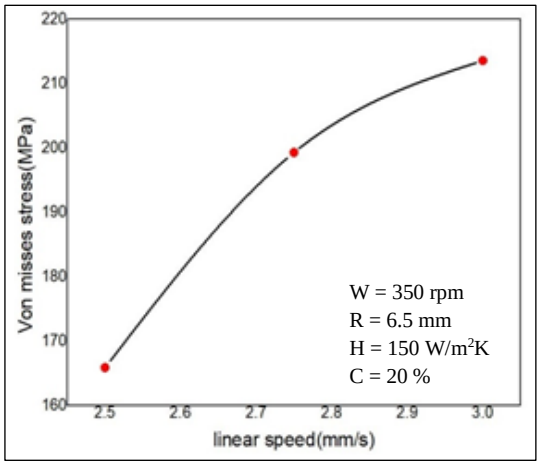

Fig. 13 von misses stress with linear speed.

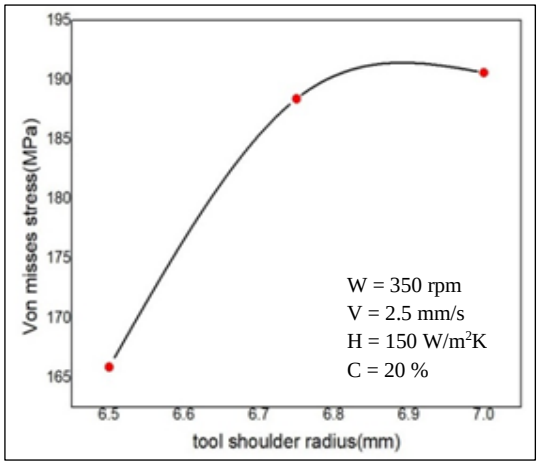

Fig. 14 von misses stress with tool shoulder radius.

While for the increases in heat transfer coefficient the value of von misses stress will increases until reached to certain value and after that it will deceases which clear in Fig. 15.

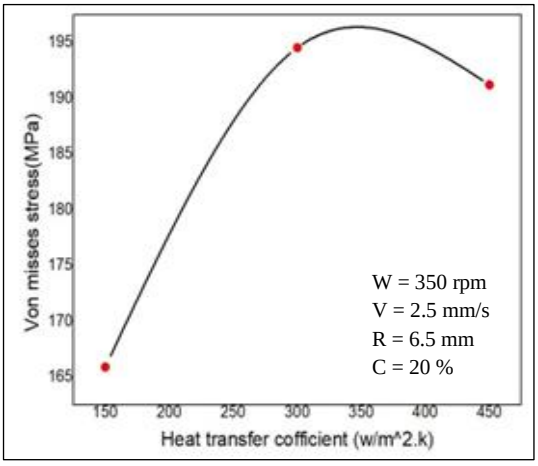

Fig. 15 von misses with heat transfer coefficient.

From the Fig. 16 it is realize that when the clamping percentage increases the value of maximum von misses stress will decreases which is a good indicator because the whole system will be more stable and the movement will prevent.

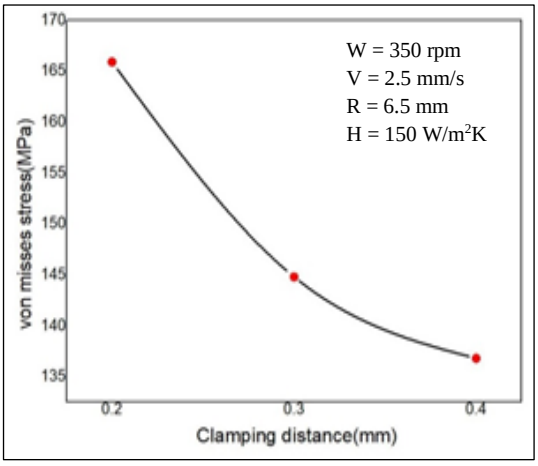

Fig. 16 von misses stress with clamping distance percentage.

For the von misses stress there is a mathematical expression with the input parameters whereby use the obtained results and apply Taguchi method for the optimization as shown in the equation (2).

$$\sigma_v = 1783 + 0.452(W) - 187(V) - 456(R) + 0.1015(H) - 1.3791(C) - 0.000192(W^2) + 42.4(V^2) + 33.8(R^2) - 0.000165(H^2) \quad (2)$$

4.1.3. Frictional stress

As fixed in the Figs. 17 and 18 when the rotational speed and heat transfer coefficient increase the value of maximum frictional stress will increases until reach to certain value and after that it will reduce, the reason of that behavior is the metal will be near to the soft phase and the friction will reduce when the rotational speed increases.

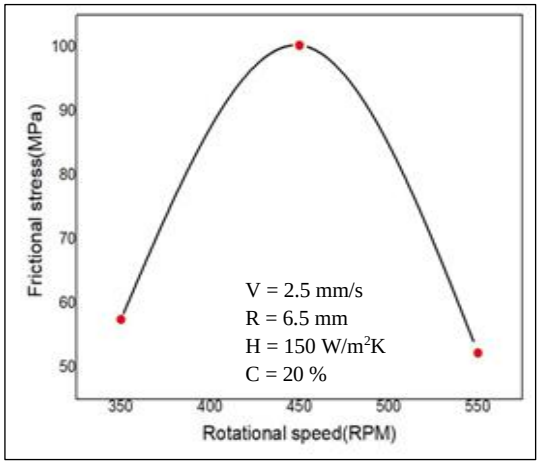

Fig. 17 frictional stress with rotational speed.

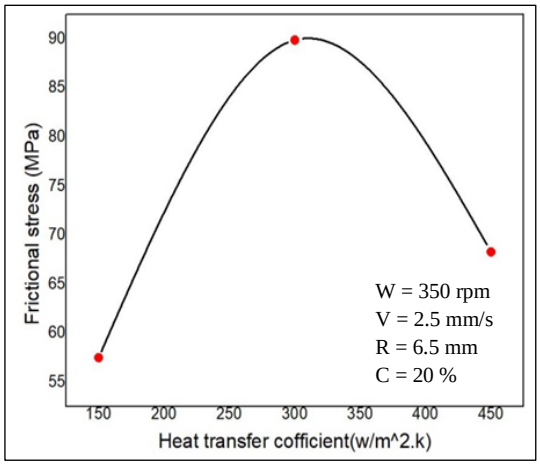

Fig. 18 frictional stress with heat transfer coefficient.

When linear tool speed increases the value of maximum frictional stress will increases while if the tool shoulder radius increases the value of maximum frictional stress will decreases and its clear in Figs. 19, and 20.

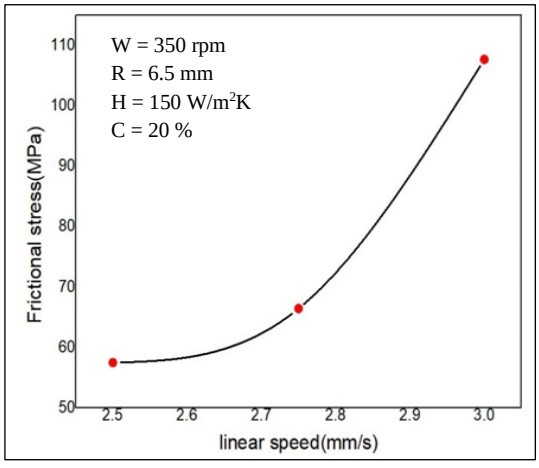

Fig. 19 frictional stress with linear speed.

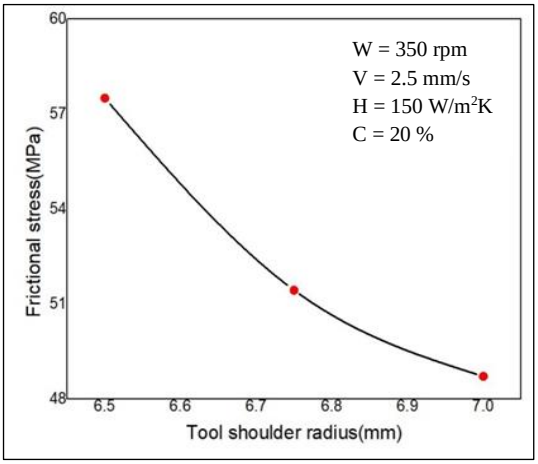

Fig. 20 frictional stress with tool shoulder radius.

Moreover, for the clamping distance percentage as increase the value of frictional stress will increase until to known value and after that will reduce as shown in Fig. 21.

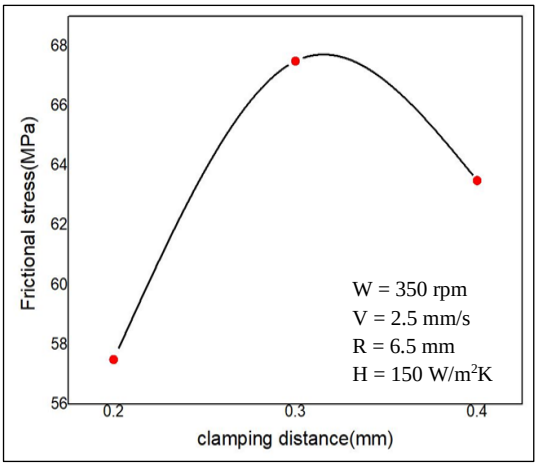

Fig. 21 frictional with stress clamping distance percentage.

Non-linear mathematical between frictional stress and input parameters was obtained by utilized FEM results and Taguchi method regression for the optimization as shown in equation (3).

$$\sigma_f = 6182 + 3.659(W) - 1732(V) - 1367(R) + 0.572(H) - 3.1(C) - 0.004089(W^2) + 330.0(V^2) + 98.6(R^2) - 0.001009(H^2) - 0.0347(C^2) - 0.00166(W \times C) - 2.93(V \times C) + 1.97(R \times C) + 0.00115(H \times C) \quad (3)$$

4.2. Optimization results

4.2.1. Temperature results

Friction stir welding process required an amount of input heat due to the friction and this heat will transform into the temperature form. The temperature distribution is more important in the welding process. Table 4 shows the ANOVA temperature.

Table 4. ANOVA for temperature.

Parameters	Sum of squares	Mean of squares	F-test	P-test
W	49388	24694	8.02	0.010
V	41549	20774.5	1.73	0.202
R	54	27	30.99	0.000
H	12273	6136.5	1.26	0.274
C	17432	8716	1.79	0.195

From the Table 4 can be see that tool shoulder radius have the most important effect on the temperature response (P = 0.000, F = 30.99) follow by the rotational speed which become in the second score of the effect on the temperature response (P = 0.01, F = 8.02) follow by the clamping percentage in the third score follow by linear speed in fourth score and at least heat transfer coefficient. Table 5 represent the optimum process parameter for the response.

Table 5. Response table for temperature.

Level	W	V	R	H	C
1	54.52	56.64	54.28	55.98	55.56
2	57.41	55.24	55.97	56.75	56.04
3	56.10	56.16	57.79	55.3	56.44
Delta	2.89	1.4	3.51	1.45	0.88
Rank	2	4	1	3	5

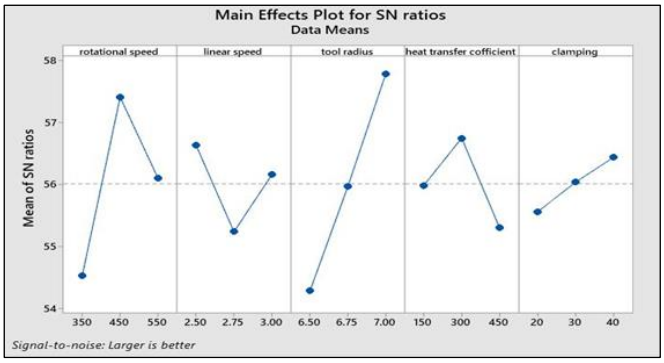

Fig. 22 Main effect plot for temperature.

From Table 5 and Fig. 22 when the rotational speed 450 rpm, welding speed 2.75 mm/s, tool shoulder radius 7 mm, heat transfer coefficient 300 W/m^2 K and clamping percentage 40 % optimum value of the temperature response can be obtained.

4.2.2. Von misses stress results

Von misses stress considers one of the most effect response during friction stir welding proses and this type of stress could be generated during the heating and cooling of the work plate material, therefor to know the effect each input parameter on this response Table 6 represents ANOVA table for von misses stress.

Table 6. ANOVA for von misses stress.

Parameter	Sum of square	Mean of square	F-test	P-test
W	40.1	20.05	643.4	0.000
V	102.3	51.15	109.35	0.000
R	10.6	5.3	0.02	0.885
H	3.1	1.55	0.17	0.709
C	3423.5	1711.75	157.15	0.000

From the Table 6, the most important effect parameter on the von misses stress was the rotational speed (P = 0.00, F = 643.4) follow by the clamping percentage which become. In the second score of the effect on the von misses stress response (P = 0.000, F = 157.15) follow by the welding speed in the third score follow by heat transfer coefficient in fourth score and at least tool shoulder radius. Table 7 represent the optimum process parameter for the response.

Table 7. Response for von misses stress.

Level	W	V	R	H	C
1	-44.09	-44.95	-45.44	-45.33	-46.11
2	-45.58	-45.39	-45.38	-45.58	-45.43
3	-46.69	-46.04	-45.55	-45.46	-45.43
Delta	2.6	1.09	0.17	0.25	1.28
Rank	1	3	5	4	2

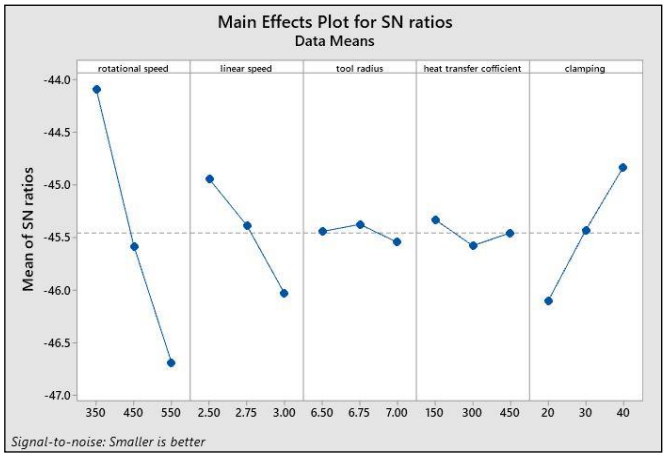

Fig. 23 Main effect plot for von misses stress.

From Table 7 and Fig. 23 it can achieved that optimum value of von misses stress (minimum value) at rotational speed 550 rpm, welding speed 3 mm/s, tool shoulder radius 7 mm, heat transfer coefficient 300 W/m^2 K and clamping percentage 20 %.

4.2.3. Frictional stress results

Frictional stress represents type of the residual stress which generated during FSW process. As FSW is a solid-state process, this stress has a value that is not lower in general and the effect of this type of stress is more important. Also, if the FSW parameter control the minimum value of frictional stress could be achieved. Table 8 represent ANOVA for frictional stress.

Table 8. represent ANOVA for frictional stress.

Parameter	Sum of square	Mean of square	F-test	P-test
W	9359.2	4679.6	68.31	0.000
V	2302.6	1151.3	16.81	0.001
R	239.8	119.9	1.75	0.21
H	2117.3	1058.65	15.45	0.002
C	12	6	0.09	0.325

From Table 8 it is clear that the most important parameter in the first stage is rotational speed (F = 68.31, P = 0.000), welding speed. In the second stage (F = 16.81, P = 0.001), heat transfer coefficient in the third stage (F = 15.45, P = 0.002), tool shoulder radius in the fourth stage (F = 1.75, P = 0.21) and clamping percentage in the final stage (F = 0.09, P = 0.525). Table 9 show the optimum process parameter for the response.

Table 9. the optimum process parameter for the response.

Level	W	V	R	H	C
1	-36.37	-38	-35.2	-35.94	-36.69
2	-39.81	-34.45	-36.29	-38.48	-36.7
3	-33.39	-37.11	-38.07	-35.15	-36.17
Delta	6.42	3.55	2.87	3.33	0.53
Rank	1	2	4	3	5

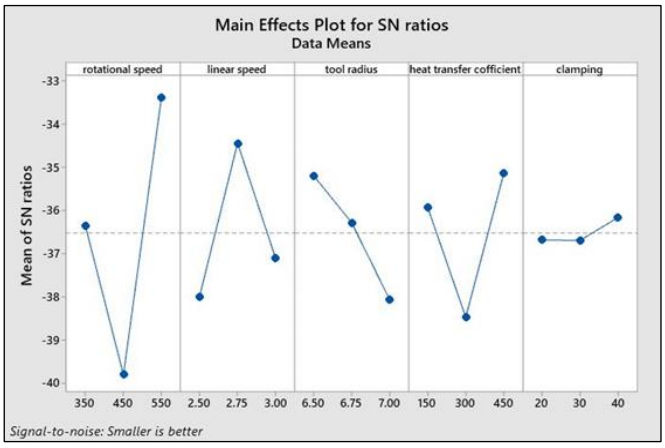

Fig. 24 Main effect plot for frictional stress.

From Table 9 and Fig. 24, the optimum parameter to obtained minimum value of frictional stress are rotational speed 450 rpm, welding speed 2.5 mm/s, tool shoulder radius 7 mm, heat transfer coefficient 300 W/m^2 K and clamping percentage 30 %.

5. Conclusions

In this paper friction stir welding process was simulate and three type of results was obtained which are the temperature, von misses stress and frictional stress with five input parameters, rotational speed, linear speed, tool shoulder radius, heat transfer coefficient and clamping percentage. There are many conclusions was achieved in this study were listed as following:

1. Maximum temperature value increase with increase in rotational speed and tool shoulder radius and clamping percentage while its decrease with increase of linear speed and heat transfer coefficient.
2. From the results it is clear that when there is an increase in the rotational speed, linear speed, tool shoulder radius, heat transfer coefficient the value of maximum von misses stress will increases but it is will decrease with the increase of the clamping percentage.
3. As the rotational speed, heat transfer and clamping percentage increases the value of maximum frictional stress will increases until it is reach to maximum value and after that deceases while frictional stress will increases with the increase in the tool linear speed but Its decreases with the increases with tool shoulder radius.

4. When the following parameter utilized, rotational speed 450 rpm, welding speed 2.75 mm/s, tool shoulder radius 7 mm, heat transfer coefficient 300 W/m^2 K and clamping percentage 40 % optimum value of the temperature response can be obtained.
5. minimum value of von misses stress can achieved at rotational speed 550 rpm, welding speed 3 mm/s, tool shoulder radius 7 mm, heat transfer coefficient 300 W/m^2 K) and clamping percentage 20 %.
6. When the following parameter are applying rotational speed 450 rpm, welding speed 2.5 mm/s, tool shoulder radius 7 mm, heat transfer coefficient 300 W/m^2 K and clamping percentage 30 %. Minimum value of frictional stress will be obtained.

References

[1] H. I. Khalaf, R. Al-Sabur, M. E. Abdullah, A. Kubit, H. A. Derazkola, "Effects of Underwater Friction Stir Welding Heat Generation on Residual Stress of AA6068-T6 Aluminum Alloy", Materials, Vol. 15, Issue 6, 2022. https://doi.org/10.3390/ma15062223

[2] R. Al-Sabur, H. I. Khalaf, A. Swierczy´nska, G. Rogalski, H. A. Derazkola, "Effects of Noncontact Shoulder Tool Velocities on Friction Stir Joining of Polyamide 6 (PA6)", Materials, Vol. 15, Issue 12, 2022. https://doi.org/10.3390/ma15124214

[3] A. S. Bahedh, A. Mishra, R. Al-Sabur, A. K. Jassim, "Machine learning algorithms for prediction of penetration depth and geometrical analysis of weld in friction stir spot welding process", Metallurgical Research & Technology, Vol. 119, Issue 3, 2022. https://doi.org/10.1051/metal/2022032

[4] R. Al-Sabur, A. K. Jassim, and E. Messele, "Real-time monitoring applied to optimize friction stir spot welding joint for AA1230 Al-alloys", Materials Today, Vol. 42, Part 5, pp. 2018-2024, 2021. https://doi.org/10.1016/j.matpr.2020.12.253

[5] M. Jayaraman, R. Sivasubramanian, V. Balasubramanian, and A. K. Lakshminarayanan, "Optimization process parameter for friction stir welding of cast aluminum alloy A319 by Taguchi method", Journal of Scientific and Industrial Research, Vol. 68, pp. 36-43, 2009.

[6] K. Gök, and M. Aydin, "Investigations of friction stir welding process using finite element method", The International Journal of Advanced Manufacturing Technology, Vol. 68, pp. 775-780, 2013. https://doi.org/10.1007/s00170-013-4798-z

[7] M. Jabbari, "RETRACTED: Elucidating of rotation speed in friction stir welding of pure copper: Thermal modeling", Computational Materials Science, Vol. 81, pp. 296-302, 2014. https://doi.org/10.1016/j.commatsci.2013.08.040

[8] G. Karrar, A. N. Shuaib, F. A. Al-Badour, N. Merah, A. K. Mahgoub, "Friction Stir Butt Welding of Commercially Pure Copper Plates", ASME International Mechanical Engineering Congress and Exposition, IMECE2014-38378, 2014. https://doi.org/10.1115/IMECE2014-38378

[9] P. K. Sahu, and S. Pal, "Multi-response optimization of process parameters in friction stir welded AM20 magnesium alloy by Taguchi grey relational analysis", Journal of Magnesium and Alloys, Vol. 3, Issue 1, pp. 36-46, 2015. http://doi.org/10.1016/j.jma.2014.12.002

[10] D. Y. Lee, K. D. Park, D. M. Kang, "A Study on the Finite Element Analysis in Friction Stir Welding of Al Alloy", Journal of the Korean Society of Manufacturing Process Engineers, Vol. 14, No. 5, pp. 81-87, 2015. http://doi.org/10.14775/ksmpe.2015.14.5.081

[11] M. A. Constantin, E. L. Niţu, and C. Bădulescu, "Numerical simulation of friction stir welding of pure copper plates", IOP Conference Series: Materials Science and Engineering, Vol. 564, 2019. https://doi.org/10.1088/1757-899X/564/1/012031

[12] R. Al-Sabur, "Tensile strength prediction of aluminium alloys welded by FSW using response surface methodology – Comparative review", Materials Today: Proceedings, Vol. 45, Part 6, pp. 4504-4510, 2021. https://doi.org/10.1016/j.matpr.2020.12.1001

[13] C. D. Sorensen, and T. W. Nelson. "Friction Stir Welding of Ferrous and Nickel Alloys", ASM International, Friction Stir Welding and Processing, pp. 111-121, 2007.

[14] H. Pashazadeh, A. Masoumi, and J. Teimournezhad, "A study on material flow pattern in friction stir welding using finite element method", Proceedings of the Institution of Mechanical Engineers, Part B: Journal of Engineering Manufacture, Vol. 227, Issue 10, pp. 1453-1466, 2013. https://doi.org/10.1177/0954405413485952

[15] S. B. Aziz, M. W. Dewan, D. J. Huggett, M. A. Wahab, A. M. Okeil, and T. W. Liao, "Impact of Friction Stir Welding (FSW) Process Parameters on Thermal Modeling and Heat Generation of Aluminum Alloy Joints", Acta Metallurgica Sinica (English Letters), Vol. 29, Issue 9, pp. 869-883, 2016. https://doi.org/10.1007/s40195-016-0466-2